Role of the QBO in modulating the influence of the 11 year solar cycle on the atmosphere using constant forcings

Katja Matthes,[1,2] Daniel R. Marsh,[3] Rolando R. Garcia,[3] Douglas E. Kinnison,[3] Fabrizio Sassi,[4] and Stacy Walters[3]

Received 26 August 2009; revised 15 April 2010; accepted 27 April 2010; published 21 September 2010.

[1] We present a set of six 20 year experiments made with a state-of-the-art chemistry-climate model that incorporates the atmosphere from the surface to the lower thermosphere. The response of the middle atmosphere to the 11 year solar cycle, its impact on the troposphere, and especially the role of an externally prescribed stratospheric quasi-biennial oscillation (QBO) is investigated with NCAR's Whole Atmosphere Community Climate Model (WACCM3). The model experiments use either fixed solar cycle inputs or fixed solar cycle together with prescribed QBO phase. The annual mean solar response in temperature and ozone in the upper stratosphere is in qualitative agreement with other modeling and observational studies and does not depend on the presence of the imposed QBO. However, the solar response in the middle to lower stratosphere differs significantly for the two QBO phases. During solar maxima a weaker Brewer-Dobson circulation with relative downwelling, warming, and enhanced ozone occurs in the tropical lower stratosphere during QBO east conditions, while a stronger circulation, cooling, and decreased ozone exists during QBO west conditions. The net ozone increase during QBO east is the combined result of production and advection, whereas during QBO west the effects cancel each other and result in little net ozone changes. Especially during Southern Hemisphere late winter to early spring, the solar response at polar latitudes switches sign between the two QBO phases and qualitatively confirms observations and other recent model studies. During a poleward downward modulation of the polar night jet and a corresponding modulation of the Brewer-Dobson circulation in time, solar signals are detected all the way down to the extratropical troposphere. Possible limitations of the model experiments with respect to the fixed solar cycle conditions or the prescribed QBO phases, as well as the constant sea surface temperatures, are discussed.

Citation: Matthes, K., D. R. Marsh, R. R. Garcia, D. E. Kinnison, F. Sassi, and S. Walters (2010), Role of the QBO in modulating the influence of the 11 year solar cycle on the atmosphere using constant forcings, *J. Geophys. Res.*, *115*, D18110, doi:10.1029/2009JD013020.

1. Introduction

[2] It has been shown in many observational and modeling studies since the end of the 1980s that the 11 year solar cycle has an impact on the chemical, thermal, and dynamical structure of the atmosphere [e.g., *Gray et al.*, 2010]. The direct radiative changes in the upper stratosphere can lead to indirect dynamical changes throughout the atmosphere [*Kodera and Kuroda*, 2002; *Matthes et al.*, 2003, 2004, 2006]. The main focus of the above mentioned studies is the understanding of the mechanism for solar influence on climate. The role of the quasi-biennial oscillation (QBO) in equatorial stratospheric zonal winds in determining the response of the atmosphere to the solar cycle is one challenging topic in this solar-climate puzzle.

[3] Labitzke and van Loon have emphasized throughout their work the need to separate the atmospheric data according to the phase of the QBO in winter [*Labitzke*, 1987; *Labitzke and Van Loon*, 1988; *van Loon and Labitzke*, 2000; *Labitzke*, 2001; *Labitzke et al.*, 2006], as well as in summer [*Labitzke*, 2003, 2005], in order to extract a solar signal. They could only confirm the so-called Holton and Tan relationship during solar minima (winters during the west phase of the QBO tend to be cold and undisturbed, while winters during the east phase tend to be warm and disturbed [*Holton and Tan*, 1980, 1982]. They note a reversal of the Holton and Tan relationship during solar maxima [*Labitzke*, 1987; *Labitzke and Van Loon*, 1988]. It is very difficult to separate the solar and QBO signals in observations partly due to the short length of existing data sets (only two to three entire solar cycles) but also due to their nonlinear

[1]Deutsches GeoForschungsZentrum, Potsdam, Germany.
[2]Freie Universität Berlin, Berlin, Germany.
[3]National Center for Atmospheric Research, Boulder, Colorado, USA.
[4]Naval Research Laboratory, Washington, DC, USA.

0148-0227/10/2009JD013020

interactions. Further complication arises from the failure of many atmospheric circulation models to reproduce a self-consistent QBO. This limits the investigation of observed processes in the modeling world. These limitations in observational and modeling studies resulted in a number of partly contrary findings in the literature that we aim to summarize.

[4] Many studies, like those of Labitzke and van Loon, focused on the effect of the late Northern Hemisphere winter circulation, i.e., January and February, dependence on the phase of the solar cycle and the QBO. *Salby and Callaghan* [2000, 2006] confirm the Labitzke and van Loon QBO-solar cycle relationship during winter as well as the statistical significances of the results [*Salby and Callaghan*, 2004]. *Camp and Tung* [2007] note in a statistical study that the solar minimum QBO west case is the least disturbed state of the atmosphere and that either the solar maximum or the QBO east phase can disturb it in agreement with Labitzke and van Loon. However, they could not confirm the reversal of the Holton and Tan mechanism during solar maxima as noted by *Labitzke and Van Loon* [1988]. *Gray et al.* [2001a, 2001b] and *Gray* [2003] emphasize the additional importance of winds in the upper stratosphere for the development of the Northern Hemisphere (NH) winter. Most of these studies were concerned with the effect of the equatorial stratosphere on the polar stratospheric circulation. However, in recent years, there is a focus on the extent of the effects on the global mean meridional circulation. Reversed signs of the solar response at high and low latitudes in NCEP/NCAR reanalyses occur from 1948 through 2006 during the two QBO phases [*Labitzke et al.*, 2006]. In February, for the QBO west phase and solar maximum, temperature signals of +12 K are calculated at northern polar latitudes in the lower stratosphere, and over −0.5 K in the Tropics. During QBO east −4 K occur at northern polar and more than +1 K at tropical latitudes [*Labitzke et al.*, 2006]. Due to the lack of an internally generated QBO in many global atmospheric models, most modeling studies on solar influence did not deal with the QBO. In this paper we explicitly impose the QBO to test observed solar-QBO relations.

[5] Other studies report on a modulation of the QBO by the solar cycle in observations such that during solar maxima the QBO circulation is stronger, while the opposite holds true for solar minima [*Salby and Callaghan*, 2000; *Soukharev and Hood*, 2001]. However, *Hamilton* [2002] could not confirm this observed modulation with a longer 50 year data set. Similarly, the QBO period modulation with the solar cycle in a two-dimensional (2-D) model [*McCormack*, 2003] could not be confirmed with another 2-D model [*Smith and Matthes*, 2008]. Note that the modulation of the QBO phase by the solar cycle cannot be tested with the presented idealized model experiments in which the QBO is artificially prescribed.

[6] The observed annual mean solar signal in temperature and ozone in the tropics shows a distinct vertical structure with a maximum in the upper stratosphere, a relative minimum in the middle stratosphere and a secondary maximum in the lower stratosphere [*Gray et al.*, 2010]. Solar signals in the tropical upper and lower stratosphere are significant whereas larger uncertainties exist for signals in the middle stratosphere. Upper stratospheric temperatures are 1 to 1.5 K and lower stratospheric temperatures are 0.5 K warmer during solar maximum [*Randel et al.*, 2009; *Frame and Gray*, 2010].

[7] Whereas larger uncertainties and discrepancies for the different temperature data sets exist, the solar induced ozone signal derived from different independent satellite analysis shows a more consistent picture with an enhancement of 2%–4% during solar maxima at midlatitudes in the upper stratosphere above 40 km, an insignificant reduction in the low-latitude middle stratosphere between 30 and 40 km, and a secondary maximum in the lower equatorial stratosphere of 1.5%–3% around 25 km [*Lee and Smith*, 2003; *Hood*, 2004; *Soukharev and Hood*, 2006; *Calisesi and Matthes*, 2006; *Randel and Wu*, 2007; *Gray et al.*, 2010].

[8] Uncertainties in the solar signal in the middle and lower stratosphere could be related to aliasing effects with the QBO and volcanic signals [e.g., *Lee and Smith*, 2003; *Smith and Matthes*, 2008] or to aliasing effects with tropical SSTs [*Austin et al.*, 2008] and ENSO [*Marsh and Garcia*, 2007]. Note, however, that ENSO effects are irrelevant for the experiments presented here since constant, climatological SSTs are used. Volcanic signals are also excluded here to study the pure solar-QBO relationship.

[9] Recently, the discrepancy between modeling studies and observations regarding the vertical structure in the tropical solar ozone signal as shown, e.g., by *World Meteorological Organization* [2007], is improving. *Austin et al.* [2007, 2008] report that a number of different chemistry-climate models (CCMs) produce a similar vertical structure of the solar signal as found in observations [*Soukharev and Hood*, 2006]. These CCM simulations are reference simulations over the recent past (1980–2000) from the SPARC CCMVal-1 initiative [e.g., *Eyring et al.*, 2005] and include a time varying solar cycle, observed, time varying SSTs, volcanic eruptions, and the effect of enhanced greenhouse gas concentrations. Some CCMs did include an (internally generated) QBO. *Austin et al.* [2008] speculate about the contribution of time varying solar cycle and SSTs for the better agreement with observations and do not find a significant relation to the presence of a QBO. Similarly, other recent simulations with CCMs reproduce the observed vertical structure in the tropical stratosphere but only with a (prescribed) QBO and constant SSTs [*Matthes et al.*, 2007] or in a CCM with fixed solar cycle conditions and with or without internally generated QBO [*Schmidt et al.*, 2010]. It is still unclear why this vertical structure of the solar signal appears and whether it is related to nonlinear interactions or arises from contamination by other signals (QBO, tropical SSTs). Most analyses of CCM runs of the recent past use multiple linear regression analysis (MLR) and it could very well be that the MLR fails to correctly attribute variance to individual predictors that may be spuriously correlated over short records [cf. *Marsh and Garcia*, 2007].

[10] Although there is broad agreement as regard the tropical solar cycle signal, the response at high latitudes is still poorly understood. Previous GCM studies with offline-calculated ozone changes were not able to represent the dynamical feedback mechanisms related to the solar cycle (modulation of the polar night jet (PNJ) and the Brewer-Dobson circulation (BDC)) [*Matthes et al.*, 2003]. By relaxing the tropical stratospheric winds to either constant QBO east or west, *Matthes et al.* [2004, 2006] were able to partly simulate the observed poleward-downward propaga-

tion of the zonal wind anomalies during NH winter for the first time, as well as significant responses in the lower stratosphere and troposphere and changes in the mean meridional circulation.

[11] The aim of this paper is to investigate the solar signal in the atmosphere with a state-of-the-art chemistry-climate model with special focus on the role of the QBO in modulating the solar signal in the tropical and extratropical stratosphere. This is done by analyzing results from idealized model calculations where fixed solar cycle conditions only or fixed solar cycle conditions and imposed QBO phases have been implemented. Section 2 describes the model and section 3 the idealized experiments that have been especially designed to test the observed solar-QBO relations. The annual mean tropical solar signal in temperature and ozone in the two different QBO phases is analyzed with special focus on the ozone budget (section 4) and some extratropical signals including a brief description of tropospheric impacts are discussed in section 5. Section 6 discusses and summarizes the results and section 7 provides conclusions.

2. Model Description

[12] The Whole Atmosphere Community Climate Model, Version 3 (WACCM3), developed at the National Center for Atmospheric Research (NCAR), is a fully interactive Chemistry-Climate Model (CCM) extending from the Earth's surface through the thermosphere (~140 km) [*Garcia et al.*, 2007]. WACCM3 is an expanded version of the Community Atmospheric Model, Version 3 (CAM3) and includes all of the physical parameterizations of CAM3 [*Collins et al.*, 2006]. It includes a detailed neutral chemistry model for the middle atmosphere based on the Model for Ozone and Related Chemical Tracers, Version 3 (MOZART3). The mechanism represents chemical and physical processes in the troposphere through the lower thermosphere. The species included within this mechanism are contained within the O_x, NO_x, HO_x, ClO_x, and BrO_x chemical families, along with CH_4 and its degradation products [*Kinnison et al.*, 2007]. The radiatively active gases (CO_2, H_2O, N_2O, CH_4, CFC-11, CFC-12, NO, O_3) affect heating and cooling rates and therefore dynamics. Additional processes described by *Marsh et al.* [2007] include heating due to chemical reactions; a model of ion chemistry in the mesosphere/lower thermosphere (MLT) [*Roble*, 1995]; ion drag and auroral processes [*Roble and Ridley*, 1987]; and EUV and NLTE longwave radiation parameterizations [*Solomon and Qian*, 2005; *Fomichev et al.*, 1998]. The horizontal resolution used in this study is 1.9° in latitude and 2.5° in longitude.

3. Experimental Design

[13] To run WACCM under perpetual solar conditions constant values of 210 flux units for the 10.7 cm radio flux (f10.7) and 4 for the K_p index were chosen for solar maximum, while for solar minimum values of 77 units for f10.7 and 2.7 for K_p were adopted. The K_p index is a measure of geomagnetic field disturbances caused by solar particle precipitation and therefore represents the effect of solar particles in the model, e.g., occurrence of aurorae. Details of the radiation changes to account for solar variability, changes within the photolysis scheme, and the ionization and energetic particles are discussed by *Marsh et al.* [2007].

3.1. Adjustment of Equatorial Winds

[14] WACCM, like many GCMs, is not able to reproduce a realistic QBO and shows instead weak easterlies in the equatorial lower stratosphere (see discussion of Figure 2 in section 3.1.2). Other studies show that a realistic QBO can be simulated by incorporating a gravity wave parameterization in combination with sufficient spatial resolution and realistic tropical convection [e.g., *Scaife et al.*, 2000; *Giorgetta et al.*, 2002; *Shibata and Deushi*, 2005; *Giorgetta et al.*, 2006].

[15] WACCM is, however, able to simulate the main features of the stratospheric semiannual oscillation (SAO) through parameterized gravity waves, although the easterlies of the SAO are slightly stronger and the westerlies do not descend far enough compared to observations.

3.1.1. QBO Relaxation Procedure

[16] To investigate the observed interaction between the QBO/SAO and the solar cycle during winter, the equatorial zonal winds in the model were relaxed toward idealized winds. These were constructed by selecting two typical, representative 28 month sequences from rocketsonde data [*Gray et al.*, 2001b], and averaging them to obtain a mean 28 month sequence. To filter out the SAO (since WACCM has its own, generated by parameterized breaking gravity waves), the data were first deseasonalized by subtracting the long-term (average over all available data) monthly means from each month. To restore the asymmetry between the QBO east and west phase the long-term annual mean was added back afterward. A spectral analysis of the rocketsonde time series revealed that the dominant peak QBO frequency lies around 28 months, as has been also confirmed by *Pascoe et al.* [2005]. For the experiments presented in this paper two profiles of the 28 month QBO sequence were selected, one for QBO east winds in the equatorial lower stratosphere and a wind reversal at or above 10hPa (on average observed at 10 hPa/32 km) and the other one for QBO west winds (Figure 1).

[17] The relaxation of the zonal-mean wind is based on *Balachandran and Rind* [1995] and has been previously tested in the Freie Universität Berlin Climate Middle Atmosphere Model (FUB-CMAM) [*Matthes et al.*, 2004]. It extends latitudinally from 22°N to 22°S decaying with a Gaussian distribution with a half width of 10°) centered at the equator. Full vertical relaxation extends from a height range of 86 to 4 hPa with a time constant of 10 days. One model level below and above this range, the relaxation is half that strong and is zero for all other levels. This procedure constrains the equatorial winds to more realistic values while allowing resolved and parameterized waves to continue to propagate. Extension of the relaxation to higher altitudes was tested but rejected because it interfered too much with the parameterized SAO.

3.1.2. Effects of the QBO Relaxation

[18] The QBO relaxation in the stratosphere does influence the development of the SAO through filtering of parameterized gravity and resolved waves [e.g., *Garcia and Sassi*, 1999]. The annual evolution of the climatological equatorial winds before and after relaxation is shown in

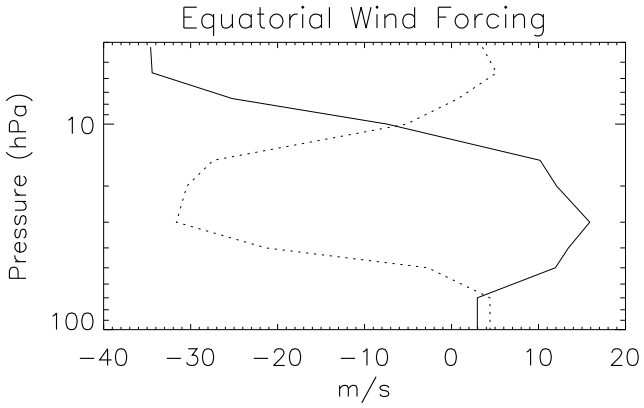

Figure 1. Mean equatorial wind profiles for QBO west (solid) and QBO east (dashed) constructed from rocketsonde data [*Gray et al.*, 2001b] that were used to constrain the zonal-mean model wind in the equatorial stratosphere to an idealized QBO (see section 3.1.1 for details).

Figures 2a–2c. Figure 2a shows the mean model case for the solar minimum experiment (min) with weak easterlies in the lower stratosphere and the SAO in the upper stratosphere. Compared to observations [e.g., *Pascoe et al.*, 2005, Figure 2] the maximum easterlies are too strong (about −60 m/s in the model and −42 m/s in observations) and the observed asymmetry between the stronger January easterlies and the weaker July easterly is not captured in the model. The magnitude of the maximum westerlies is well captured by the model, although, again, there is no asymmetry between the spring and autumn maximum. In general, the model SAO occurs at too high an altitude compared to observations; in particular, the westerlies do not descend far enough into the upper stratosphere. Figures 2b and 2c show the mean QBO east and west in the lower stratosphere with a shear zone above and the SAO in the upper stratosphere/lower mesosphere. The asymmetry between QBO east (−30 m/s) and west (+15 m/s) in the lower stratosphere is well reproduced by relaxing the model zonal winds toward observed values. Through the incorporation of the QBO in the lower stratosphere the SAO westerly phase is shifted further upward. In the case of QBO east the SAO westerlies and easterlies are stronger than for the normal case (Figure 2a). For the QBO west, gravity waves tend to break even higher and easterlies dominate the upper stratosphere. Note that the gravity wave spectrum was not adjusted after adding the QBO in order to be able to compare the runs with the already existing control runs.

3.2. Model Integrations

[19] Six 20 year equilibrium model runs were performed with WACCM3 using the above described changes in solar irradiance under constant solar maximum and solar minimum conditions, with and without constant, prescribed QBO east or west conditions in the equatorial lower stratosphere (Table 1). All experiments were integrated with an annual and diurnal cycle, constant 1995 greenhouse gas (GHG) conditions, and had a repeating climatological seasonal cycle in sea surface temperatures (SSTs); hence the effects of ocean-atmosphere feedback and the effect of enhanced GHG concentrations are neglected. The experiments presented here do not include a realistic time varying 11 year solar cycle or a realistic time varying QBO and are thus somewhat idealized similar to other existing solar cycle influence studies. Since ozone is calculated interactively in WACCM3, the ozone budget for the two QBO phases is analyzed in detail and provides a novelty compared to existing model studies.

4. Annual Mean Temperature and Ozone

[20] In this section we first show the annual mean response to the solar cycle for all experiments (Table 1) under fixed solar cycle conditions only or fixed solar cycle

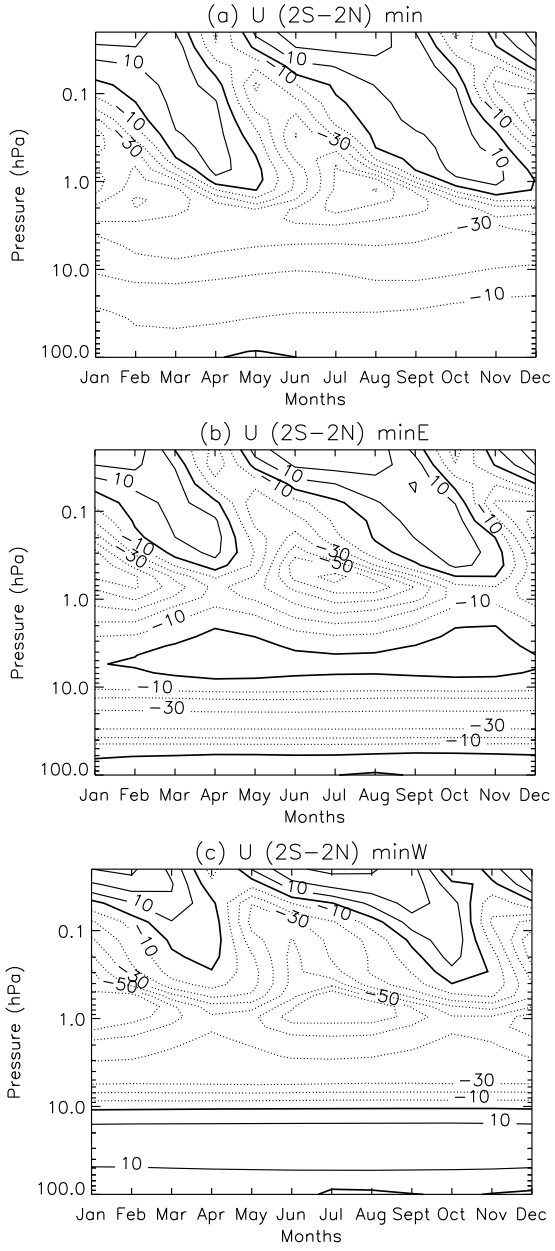

Figure 2. Twenty year monthly mean equatorial zonal-mean wind from the model (averaged from 2.8°S to 2.8°N) from January through December for (a) min, (b) minE, and (c) minW in the equatorial lower stratosphere; contour interval is 10 m/s.

Table 1. Solar-QBO Experiments Performed With WACCM Using Constant Solar and QBO Forcings

Experiment Name	Zonal Wind in Equatorial Lower Stratosphere	Solar Cycle Phase
max	standard weak east	maximum
min	standard weak east	minimum
maxW	west	maximum
minW	west	minimum
maxE	east	maximum
minE	east	minimum

conditions and fixed, imposed QBO phases. We start with the tropical signal and focus on the role of the QBO for the solar response in the stratosphere. Then the seasonal evolution of the tropical signal and its extratropical counterparts are discussed. Possible implications for the tropospheric circulation are shown. All differences between solar maxima and solar minima are based on monthly mean data, averaged over 20 model years. Statistical significances are calculated using a two-sided Student's t test.

4.1. QBO Impact on the Solar Response in Tropical Temperature and Ozone

[21] Figures 3 (top) and 3 (bottom) show the annual mean ozone and temperature differences between solar maximum and minimum, integrated between 25°S and 25°N for the QBO east experiment (solid lines), the QBO west experiment (dashed lines), and the experiment without nudged QBO (dotted lines). All three simulations yield similar values in the upper stratosphere with a maximum ozone response of 2.6% around 38 km (Figure 3, top) and a maximum temperature response of 0.7 K at around 43 km (Figure 3, bottom) as expected from the direct solar UV effect on shortwave heating rates and hence on temperature and ozone. The three simulations start to differ below 35 km and especially below 25 km, where dynamical interactions and transport processes become important.

[22] Whereas a distinct ozone minimum response (1.3%) exists for the QBO east experiment around 29 km, the ozone response steadily decreases below the upper stratospheric maximum for the QBO west experiment and the experiment without nudged QBO. A similar response is seen for the temperature. Statistically significant differences exist for the QBO east and the QBO west experiment in the lower stratosphere. The QBO east experiment shows a maximum response of up to 2.8% around 18 km whereas the QBO west experiment reaches only 0.6%. Note that in the height region between 20–25 km where the largest ozone column changes occur, the differences between the two QBO phases are smaller and reach approximately 1.5 % for QBO east and 0.5% for QBO west. The ozone response in the case without nudged QBO lies in between the two QBO cases. Similar results are obtained for the temperature response: whereas the QBO east experiments show a maximum of 0.4 K around 20 km (slightly higher than the maximum ozone response), the response in the QBO west experiment is less than 0.1 K.

[23] Although the model results in particular the QBO east experiments show qualitative agreement with observations, with maxima in the upper and lower stratosphere and a relative minimum in the middle stratosphere in the solar ozone and temperature signals, they differ in the magnitude and sometimes also the height of the response. While the observed upper stratospheric maximum reaches 2.8% at 43 km in the SAGE I+II data [*World Meteorological Organization*, 2007], all three sets of experiments show a similar maximum but at somewhat lower altitudes (38 km). Note that the model response in the upper stratosphere does not depend on the presence of the imposed QBO, while the solar response in the middle and lower stratosphere shows significantly different responses for the two QBO phases.

[24] Modeled annual mean solar temperature signals are smaller than the observed responses of about 1 K in the upper stratosphere [*Randel et al.*, 2009] and more than 1 K for the QBO east and 0.5 K for the QBO west in the lower stratosphere [*Labitzke*, 2005]. Similarly, the observed solar ozone response unstratified by QBO phase is about 2% in the tropical stratosphere [*Soukharev and Hood*, 2006; *Randel and Wu*, 2007], while the mean response in the model simulations is about 1% in this region.

[25] In summary, we find that the WACCM3 model solar response in the middle and lower stratosphere depends on the phase of the QBO, and that the QBO east experiment agrees qualitatively with observations that are not separated according to the QBO. In what follows, we test and explore further the role of the QBO in modulating the solar signal.

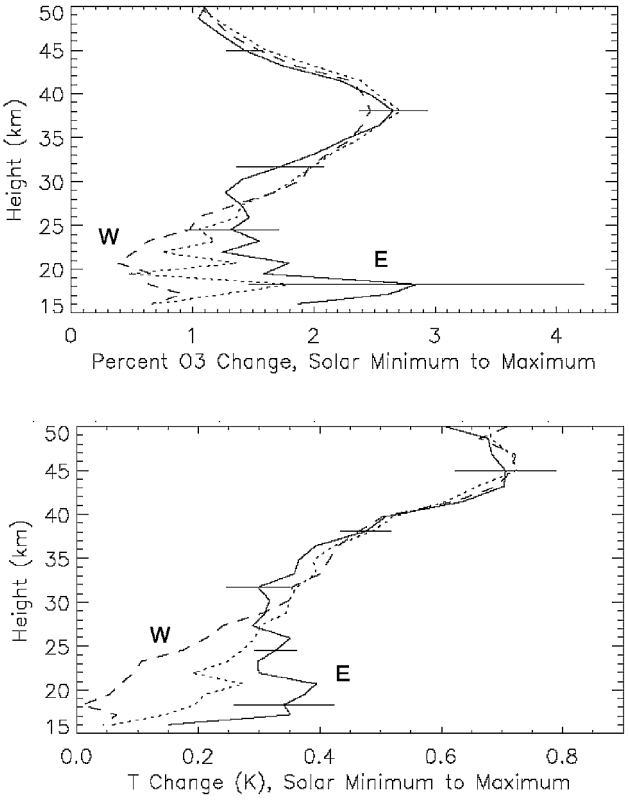

Figure 3. (top) Ozone differences between solar maximum and solar minimum in percent for the QBO east experiment (solid, maxE minus minE) with 2σ error bars for selected heights, the QBO west experiment (dashed, maxW minus minW), and the solar cycle-only experiment (dotted, maximum minus minimum) for the tropics (averaged from 25°S to 25°N). (bottom) Same as Figure 3 (top) but for the temperature differences in K.

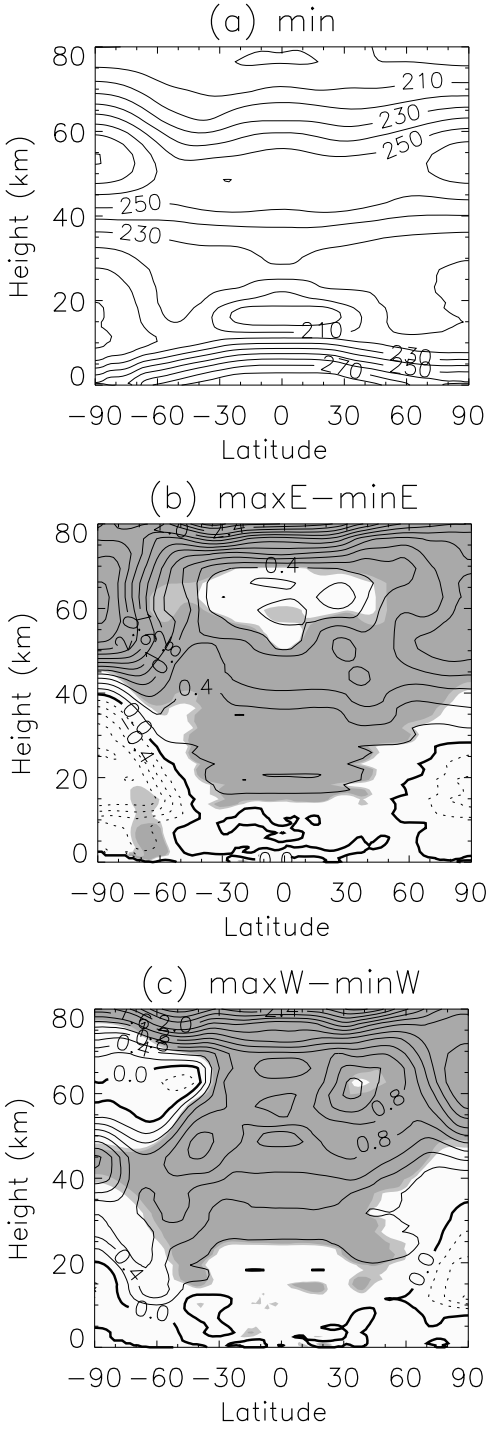

Figure 4. (a) Twenty year annual mean temperature distribution in Kelvin (K) from 0 to 80 km in the minE experiment with a contour interval of 10 K. (b) Temperature differences for the QBO east experiment (maxE minus minE) with a contour interval of 0.2 K. Light and dark shading indicates the 90% and 95% significance level from a two-tailed Student's *t* test. (c) Same as Figure 4b but for the QBO west experiment (maxW minus minW).

4.2. QBO Impact on the Latitude-Height Structure of the Solar Signal

[26] The annual mean latitude-height structure of the solar signal in temperature and ozone from the Earth's surface up to 80 km is presented in Figures 4 and 5. We note that the annual mean direct temperature response around the equatorial stratopause for both QBO cases (Figures 4b and 4c) corresponds with a maximum in shortwave heating rate (not shown) and agrees with other modeling studies [e.g., *Brasseur*, 1983; *Matthes et al.*, 2003, 2004; *Schmidt and Brasseur*, 2006; *Marsh et al.*, 2007; *Schmidt et al.*, 2010]. The maximum in the models is, however, smaller than in observations, although the observations themselves do diverge as discussed in the section 1. Note that in many published observational and modeling studies the solar response is not stratified according to the phase of the QBO for the annual mean, nor is the response shown for the entire vertical domain from the ground to the lower mesosphere. The solar temperature response in the middle and lower stratosphere at 20 km reaches 0.4 K in the tropics in the QBO east, but only 0.05 K in the QBO west experiment, in qualitative agreement with *Labitzke* [2005, Figure 8].

[27] In general, significant positive temperature differences exist in the tropical and subtropical stratosphere that extend further into the lower stratosphere for the QBO east and are shifted toward midlatitudes in the QBO west case. Slight positive, but mostly insignificant temperature differences occur down to the troposphere and the Earth's surface from 50°S to 50°N. In the QBO east case a pattern of partly statistically significant, negative temperature differences exists in both hemispheres poleward of 50° in the troposphere and lower stratosphere, reaching even into the upper stratosphere in the SH. The solar signal in the SH is reversed but insignificant for the QBO west case. The solar signals at polar latitudes are mostly not statistically significant because dynamical variability overwhelms them. A nonsignificant relative minimum occurs in the QBO east case in the mesosphere (65 km) above the equatorial stratospheric maximum whereas a reversed signal, i.e., a significant relative maximum, appears for the QBO west case.

[28] Independent of the presence of a prescribed QBO, the solar temperature response above 70 km is statistically significant and positive and increases with height due to larger absorption of radiation at shorter wavelengths (EUV) during solar maxima. A maximum solar temperature response of about 2 K can be found at the equator, at 80 km height. Note that the temperature response continues to increase with height to the lower thermosphere (not shown).

[29] The corresponding annual mean O_3 changes from solar minimum to maximum for the QBO east and west experiments are shown in Figure 5. The solar ozone response for the two QBO phases between 30 and 50 km shows similar behavior to the solar temperature response discussed above (Figure 4). During solar maximum, very symmetric, statistically significant ozone increases are obtained from the tropics to the midlatitude upper stratosphere (maximum at 40 km) of 2%–3%, in good agreement with observations and previous modeling studies that do not separate according to the phase of the QBO [e.g., *Brasseur*, 1983; *Haigh*, 1994; *Fleming et al.*, 1995; *Shindell et al.*, 1999; *Schmidt and Brasseur*, 2006; *Marsh et al.*, 2007].

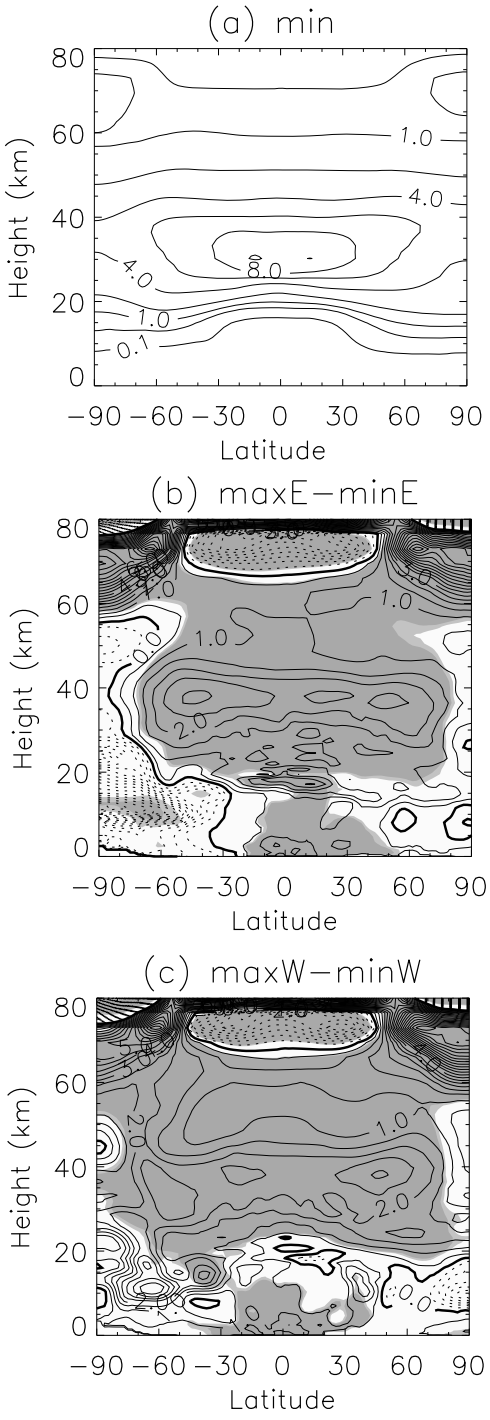

Figure 5. (a) Twenty year annual mean ozone distribution in part per million by volume (ppmv) from 0 to 80 km in the minE experiment with a contour interval of 1 ppmv. (b) Ozone differences for the QBO east experiment (maxE minus minE) with a contour interval of 0.5%. (c) Same as Figure 5b but for the QBO west experiment (maxW minus minW). Shading as in Figure 4.

Below 30 km strikingly different solar ozone responses are calculated in the two phases of the QBO in the tropics and in the extratropics. In the lower stratosphere, where the secondary maximum in solar ozone response occurs for the QBO east experiment, water vapor does increase by about 3% as well (not shown). Significant solar ozone anomalies exist for the QBO east and west experiment in the tropical to midlatitude troposphere.

[30] Above about 50 km the response to the solar cycle is almost identical in both QBO phases. The ozone anomalies in the upper atmosphere and especially the statistically significant ozone decrease of 3% throughout the tropical and subtropical mesosphere can be explained by the enhanced H_2O photolysis due to increased irradiance in the Lyman α line. The ozone increase of 10% in the midlatitude and high-latitude mesosphere (~70 km) occurs right at the location of the tertiary ozone maximum [*Marsh et al.*, 2001] and is related to the chemistry of the region. The annual mean solar temperature and ozone response in the upper stratosphere agrees well with a set of 30 year equilibrium simulations of WACCM with a different (coarser) horizontal resolution [*Marsh et al.*, 2007], and also with a recent simulation with a model comparable to WACCM, i.e., the HAMburg Model of the Neutral and Ionized Atmosphere (HAMMONIA) [*Schmidt and Brasseur*, 2006; *Schmidt et al.*, 2010]. The vertical structure of the temperature and ozone response in the tropical middle and lower stratosphere is reproduced by *Schmidt et al.* [2010] regardless of an (internally generated) QBO but not by *Marsh et al.* [2007] where no imposed QBO was present. We conclude that at least in WACCM the vertical structure of the tropical solar signal in the presented set of experiments is due to the (prescribed) QBO.

5. Seasonal March of the Signals

5.1. Lower Stratosphere: Tropics Versus Extratropics

[31] So far only annual mean results have been presented. In this section we will investigate the seasonal evolution of the response to solar variability in the lower stratosphere in the QBO east compared to the QBO west experiment. To explore the different response in the two QBO phases in the tropical lower stratosphere and investigate whether they are related to extratropical circulation changes, Figures 6 (QBO east) and 7 (QBO west) show latitude-time sections of deseasonalized temperature (Figures 6a and 7a) and ozone anomalies (Figures 6b and 7b) as well as deseasonalized anomalies of the Transformed Eulerian Mean (TEM) vertical velocity, ($\overline{w}^*$), averaged over the lower stratosphere (100–30 hPa) (Figures 6c and 7c).

[32] In the QBO east experiment (Figure 6a), positive solar temperature signals (0.2–0.3 K) exist between 30°N and 30°S throughout the year, that are statistically significant from January to July. Corresponding negative solar temperature responses exist at high latitudes, statistically significant from January through September at southern mid to high latitudes only. The solar ozone responses (Figure 6b) show a very similar pattern to the solar temperature signals with statistically significant positive values of about 1%–1.5% in the tropics and subtropics throughout the year. At higher latitudes there are statistically significant responses during part of the year, which are negative in the Southern Hemisphere but positive in the Northern Hemisphere.

[33] In the QBO west experiment (Figures 7a and 7b) weak, nonsignificant signals in temperature and ozone are found in the Tropics, whereas a stronger and partly statis-

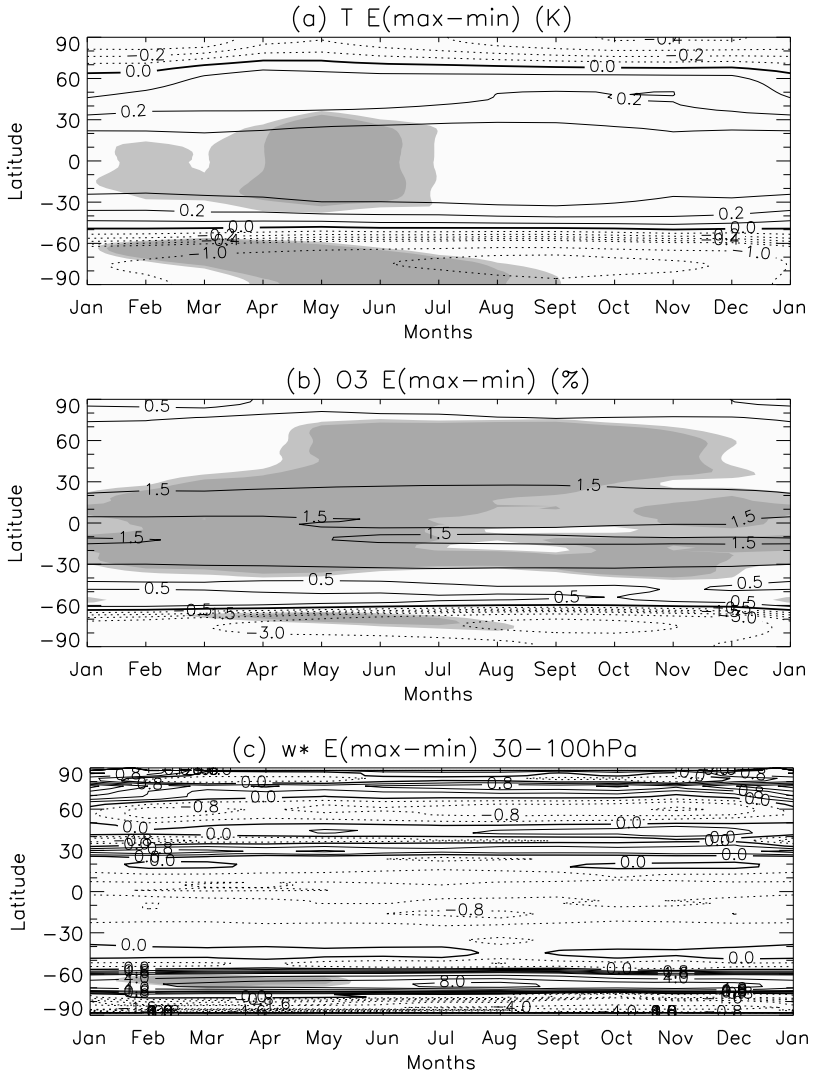

Figure 6. Deseasonalized monthly mean latitude-time sections integrated over the lower stratosphere (between 100 and 30 hPa) from January through December of the QBO east experiment (maxE minus minE) for (a) the temperature differences with a contour interval of 0.1 K, (b) the ozone differences with a contour interval of 0.5%, and (c) the differences in the vertical component of the TEM circulation $\overline{w}^*$ in mm/s multiplied by 100 with contour intervals of ±0, 0.4, 0.8, 1.2, 1.6, 2, 4, 6, 8, 10, and 12. Shading denotes statistical significances as in Figure 4.

tically significant positive solar signal occurs in mid to high latitudes. Even though clear and opposite solar signals exist during SH winter for the QBO east and the QBO west experiments, the solar signals during NH winter are not distinguishable for the two QBO phases.

[34] The anomalies for the two QBO phases suggest a response of the global mean circulation to the solar cycle such that there is relative sinking motion and adiabatic warming at low latitudes and relative ascending motion associated with cooling at southern high latitudes during the east phase of the QBO. The reverse holds true for the west phase of the QBO. Changes in $\overline{w}^*$ in Figures 6c and 7c are broadly consistent with the picture inferred from solar temperature and ozone anomalies and suggest a weakening of the Brewer-Dobson circulation for the QBO east and a strengthening for the QBO west experiment during solar maxima. However, these changes are not statistically significant.

5.2. Contribution of Production, Advection, and Loss to the Solar Cycle Signal in Ozone in the Tropical Lower Stratosphere

[35] To investigate in more detail solar induced ozone signals in the tropical lower stratosphere for the two QBO phases (Figure 3), we evaluate the contribution of ozone production (P), advection (A) and photochemical lifetime (τ) to annual mean changes in ozone during solar maximum and minimum. The importance of chemical production, advection and chemical loss cycles on ozone depends strongly on altitude. The main photochemical production mechanism for ozone, the photolysis of molecular oxygen,

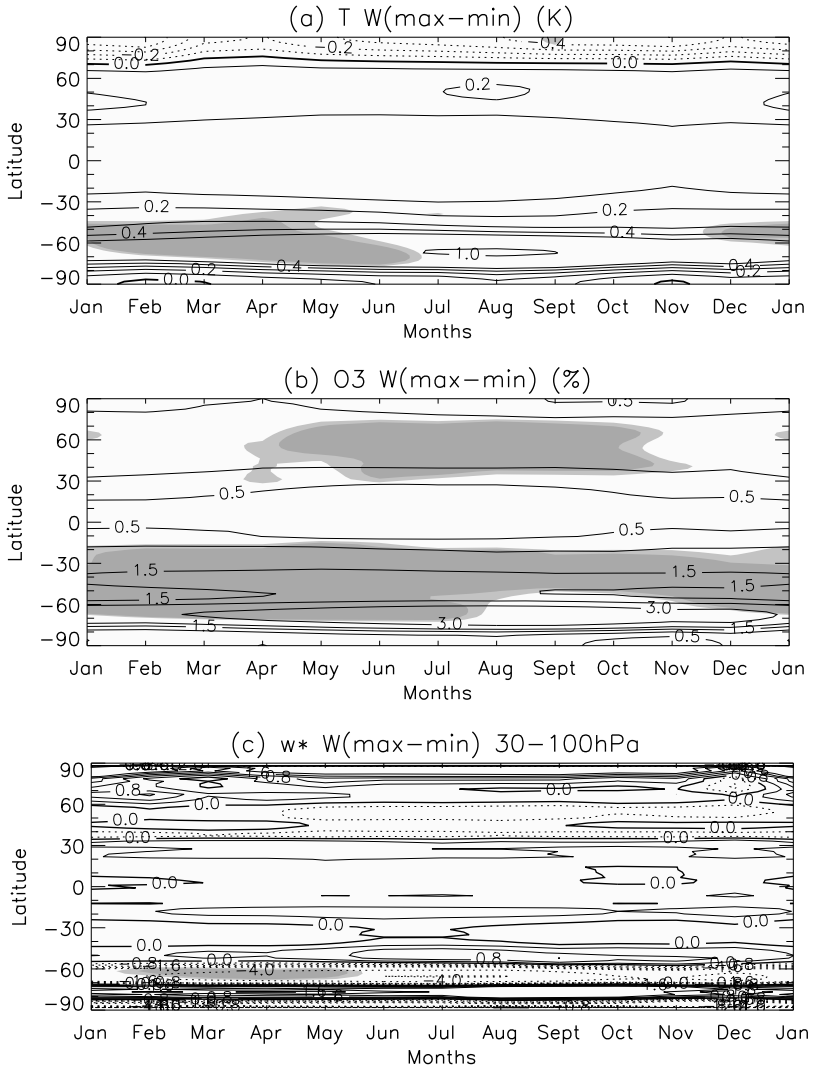

Figure 7. Same as Figure 6 but for the QBO west experiment.

peaks in the tropics with a maximum around 40 km [e.g., *Brasseur and Solomon*, 2005]. Several catalytic cycles involving the O_x, NO_x, HO_x, ClO_x, and BrO_x chemical families are fast sinks of ozone above 30 km. Below 30 km, the rates of both production and loss slow markedly, so that advection becomes important in establishing the equilibrium ozone concentration. To estimate quantitatively the fractional difference in ozone, $\delta O_3/O_3$, between solar maximum and solar minimum we follow *Tilmes et al.* [2009] and evaluate the terms in the ozone continuity equation averaged over the annual cycle and between latitudes ±25° for both QBO phases separately:

$$0 \approx P + A - \frac{O_3}{\tau}, \tag{1}$$

where P and A denote production and advection, respectively; photochemical loss is represented by the term $-O_3/\tau$, where τ is the chemical lifetime; and the time tendency of ozone vanishes on annual averaging. Then, as shown by *Tilmes et al.* [2009], the fractional ozone difference between solar minimum and solar maximum can be written as

$$\frac{\delta O_3}{O_3} = \frac{\delta(P+A)}{(P+A)} + \frac{\delta\tau}{\tau}, \tag{2}$$

where only terms linear in δO_3, δP, and $\delta\tau$ are retained. In the tropical stratosphere the transport term, A, is dominated by vertical advection, $-w^*\partial O_3/\partial z$ (something which we have verified from model results). For the simulations used in this study, we have monthly mean output for w^* and $\partial O_3/\partial z$, but not for their product, so calculating $A = -w^*\partial O_3/\partial z$ from the monthly mean vertical velocity and vertical ozone gradient is subject to inaccuracies as it neglects transient contributions. For this reason, we have not calculated A directly, but instead assigned to it the value necessary to balance equation (1) at each altitude.

[36] In Figure 8 we show each term of equation (2) for solar max and solar min conditions in the tropics (averaged between 25°S and 25°N) for QBO east and QBO west. In

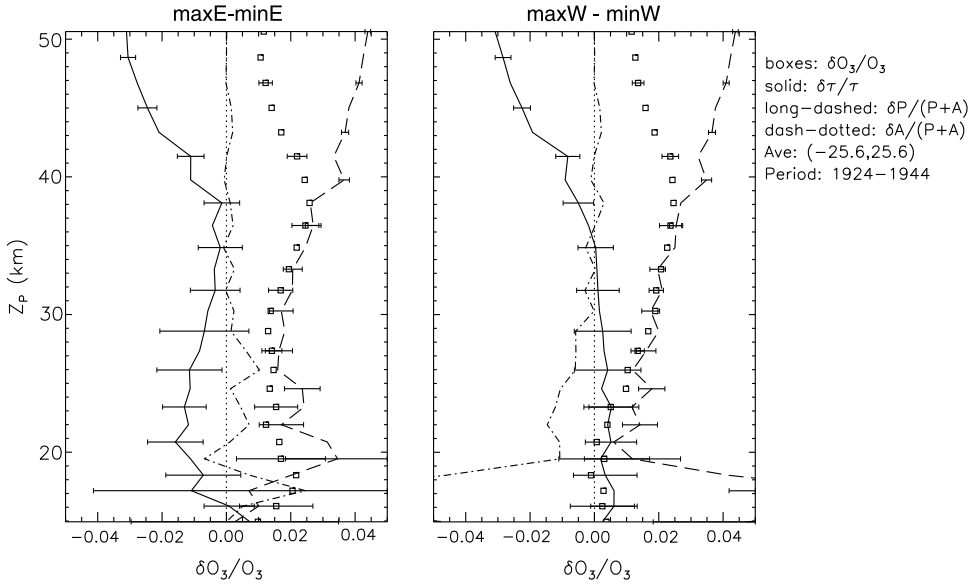

Figure 8. Fractional change of ozone, $\delta O_3/O_3$, (squares) between solar minimum and solar maximum for (left) the QBO-east experiment (maxE minus minE) and (right) the QBO-west experiment (maxW minus minW). The contributions to $\delta O_3/O_3$ from fractional changes in O_x chemical lifetime (solid lines), O_x production rate (dashed lines), and advection (dash-dotted lines) are also shown. Two-sigma uncertainties are indicated by the error bars, except for the fractional advection term, which was not calculated directly. See section 5.2 for details.

both cases, changes in production (P) and lifetime (τ) account for essentially all of the fractional change in ozone above 30 km, as expected from the fact that ozone is in photochemical equilibrium at these altitudes. Below 30 km, advection is not negligible in either phase of the QBO. In QBO east, however, the effect of advection is relatively small, and there is a net increase in ozone at all altitudes below 30 km, peaking in the lowermost stratosphere, near 18 km. In contrast, during QBO west changes in production and advection dominate the contributions to the fractional change in ozone below 30 km. In the lowermost stratosphere, below 20 km, both P and A make large, but canceling, contributions. Thus, there is little net change in $\delta O_3/O_3$ between solar max and min in the QBO west

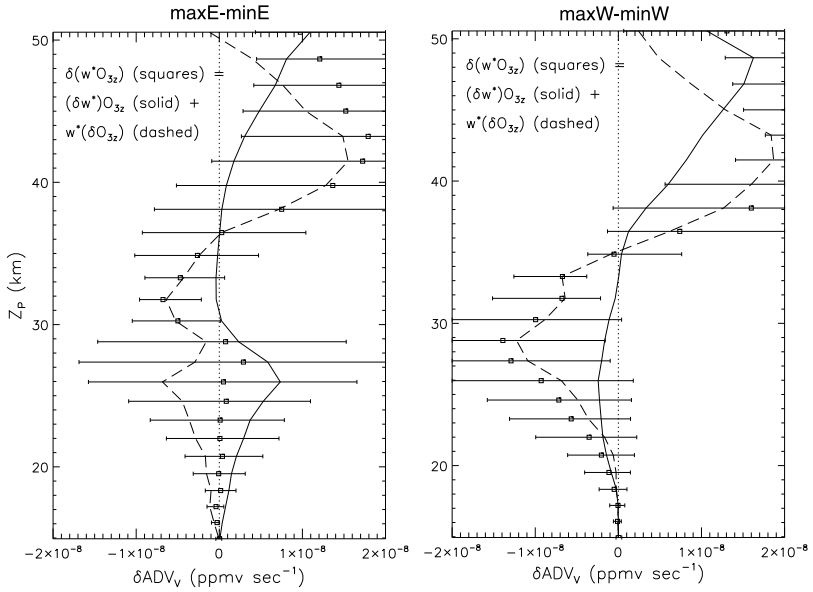

Figure 9. Change in vertical advection of ozone, $-w^*\partial O_3/\partial z$, between solar minimum and solar maximum (squares) for (left) QBO-east and (right) QBO-west, together with the contribution from changes in vertical velocity (solid lines) and changes in the vertical gradient of ozone (dashed lines). See section 5.2 for details.

experiment below 20 km, even though the fractional changes in production and advection are individually much larger than in the QBO east experiment.

[37] Figure 9 provides some insight into the different role played by advection under QBO east and QBO west conditions. Figure 9 shows tropical and annual averages of the change in $-w^*\partial O_3/\partial z$ between solar minimum and solar maximum for QBO east (Figure 9, left) and QBO west (Figure 9, right). In addition, the total change in $-w^*\partial O_3/\partial z$ is broken up into contributions due to changes in vertical velocity and vertical ozone gradient, as follows:

$$\delta\left(-w^*\frac{\partial O_3}{\partial z}\right) = -\delta(w^*)\frac{\partial O_3}{\partial z} - w^*\delta\left(\frac{\partial O_3}{\partial z}\right). \quad (3)$$

[38] The two terms on the RHS of equation (3) are indicated in Figure 9 by the solid and dashed curves, respectively. During QBO east, the total change in $-w^*\partial O_3/\partial z$ is small below 30 km, as already seen in Figure 8. According to Figure 9, this occurs because the two contributions to $-w^*\partial O_3/\partial z$ tend to cancel each other. This is what we expect from our calculations for QBO east, where w^* decreases from solar minimum to solar maximum (see Figure 6), while $\partial O_3/\partial z$ increases due to enhanced production of ozone at solar maximum. This situation makes the first term on the right-hand side of (3) positive, while the second term remains negative, leading to the cancelation illustrated in Figure 9 (left). In QBO west, on the other hand, w^* increases between solar minimum and solar maximum (Figure 6) and so does $\partial O_3/\partial z$. Both terms on the right-hand side of equation (3) are therefore negative and reinforce each other in this case, as seen in Figure 9 (right).

[39] The foregoing analysis implies that the annual-mean ozone mixing ratio in the lower stratosphere must be controlled by a delicate balance of terms (advection, production, loss) that are all very small but of comparable magnitude since (in the absence of secular change) there can be no net tendency of ozone over the annual cycle. Thus the small but opposite signed changes in w^* in the QBO east versus the QBO west experiment will dictate the solar cycle signal in ozone in the lower stratosphere because, as a consequence of these changes, advection is ineffective in counteracting changes in production in QBO east, but quite effective in doing so in QBO west. This results in the behavior seen in Figure 8, where increases in ozone production lead to a net ozone increase between solar minimum and solar maximum in QBO east, but are opposed by changes in advection in QBO west, such that no net ozone increase occurs in that phase. Incidentally, the very large increases in ozone production below 20 km in QBO west (Figure 8, right) should be viewed as a consequence of the fact that in QBO west there are only small changes in ozone in the 20–25 km range, so there is no increase in ozone overburden to interfere with increased production.

[40] It should also be noted that solar cycle changes in ozone are very small in absolute terms for both QBO east and QBO west. The analysis presented in Figure 8 (and the results shown in Figure 3) are all fractional, or percentage, changes. While the largest such changes are comparable in the upper and lower stratosphere during QBO east (~2.5%), the absolute changes in ozone mixing ratio are much larger near the ozone mixing ratio maximum in the middle stratosphere (~30 km), where the mixing ratio is over a factor of 10 larger than in the lowermost stratosphere. This statement holds even as regards ozone concentration (molecules/cm^3), since the latter is some four times larger at 30 km than at 18–20 km.

[41] There remains the question why the solar cycle response of w^* is of opposite sign in QBO east versus QBO west in the simulations presented here. We do not have a definitive answer to this question but the results shown in section 5.3 suggest that the strength of the Brewer-Dobson circulation decreases between solar minimum and solar maximum in QBO east and increases in QBO west years. The observed solar signal in tropical, lower stratosphere ozone is qualitatively reproduced by our simulations, thus one may infer that the real Brewer-Dobson circulation behaves in a similar manner.

5.3. Extratropical Response in Zonal-Mean Wind and Temperature

[42] Figure 10 shows a comparison of the temperature and zonal-mean zonal wind signals in the SH between the east and the west phase of the QBO from June to October where the largest solar induced anomalies occur in the tropical lower stratosphere at high latitudes (Figures 6 and 7). In June and July, the temperature differences for both QBO phases are characterized by a statistically significant warming of the tropical and subtropical upper stratosphere during solar maxima due to increased absorption of UV radiation (Figures 10b and 10d). In the early part of the winter the stratosphere is still under radiative control and therefore very sensitive to these direct solar changes that provide an additional thermal forcing [*Kodera and Kuroda*, 2002].

[43] For the QBO east case, the solar induced temperature differences in the tropics extend to the lower stratosphere with time, leading to the secondary temperature maximum (see Figure 6a). In the QBO west case however, the significant tropical warming is confined to the upper stratosphere and mesosphere whereas weaker, nonsignificant anomalies dominate the lower stratosphere and upper troposphere (Figure 10d). At high latitudes a strengthening and downward extension of the temperature anomalies appears that maximizes in September for both QBO cases and forms a mostly statistically significant characteristic quadrupole pattern with reversed signs for the two QBO phases. The largest solar induced wind and temperature anomalies appear in September during the late winter to early spring period that is most susceptible for planetary wave forcing. Note that significant anomalies reach the ground in the QBO east but not the QBO west case.

[44] Corresponding to the quadrupole anomalies in temperature that are strongest in September, a dipole pattern in the zonal-mean zonal wind anomalies exists at high southern latitudes that reach +10 m/s at 40 km for QBO east (Figure 10a) and −8 m/s at 40 km for QBO west (Figure 10c). These anomalies grow and propagate poleward and downward from the subtropical stratopause region. This modulation of the polar night jet is also seen in observations [*Kuroda and Kodera*, 2002] although the maximum response occurs in August in the SH whereas it appears one month later in WACCM3. The later appearance in

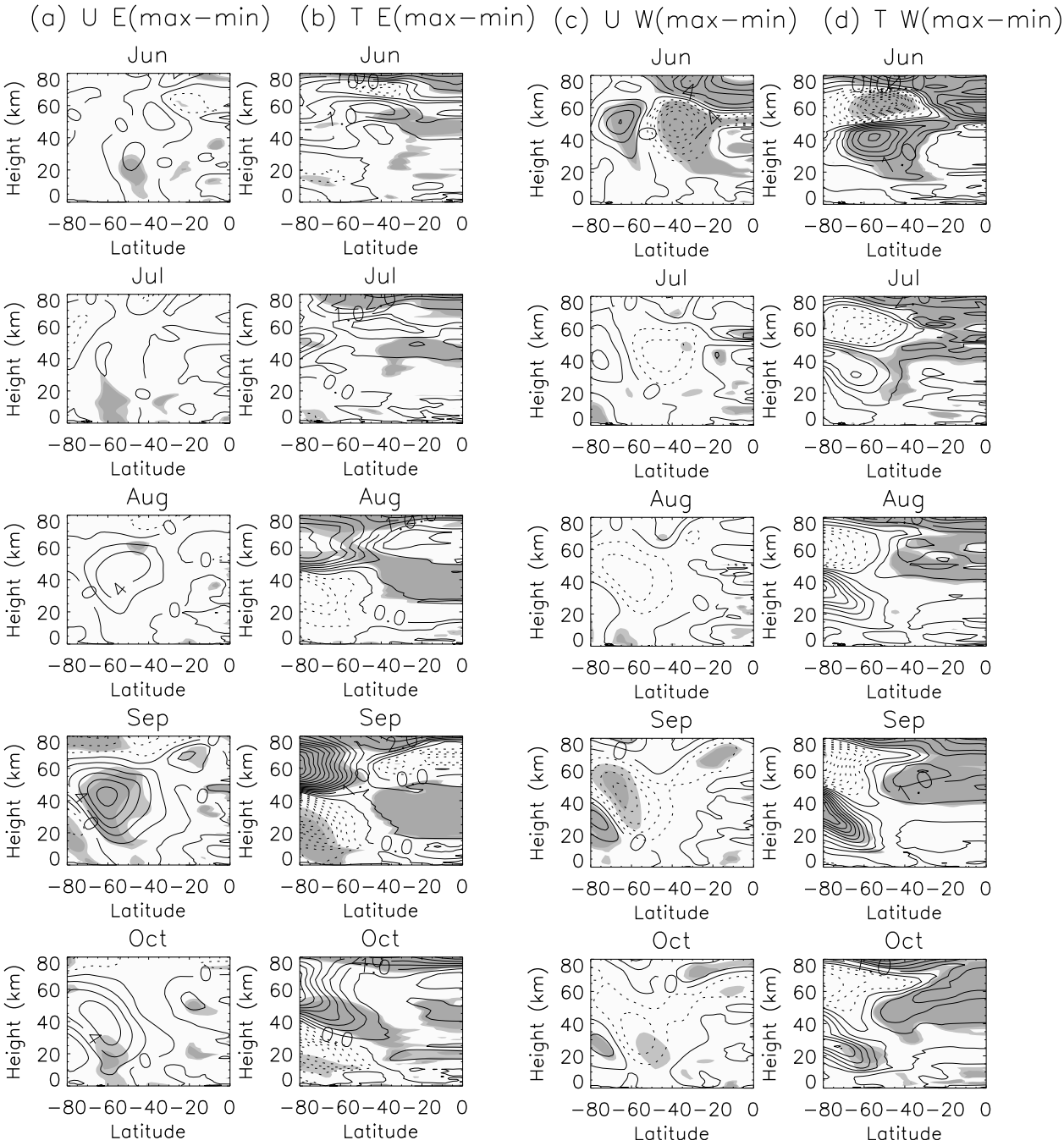

Figure 10. June through October temperature and zonal-mean zonal wind differences between solar maximum and minimum for the (a and b) QBO east (maxE minus minE) and (c and d) QBO west (maxW minus minW) experiments; shading as in Figure 4.

WACCM3 is probably related to the unrealistic long winter season.

5.4. Response in Wave-Mean Flow Interactions

[45] Since the solar induced poleward-downward modulation of the polar night jet in time involves refraction of planetary waves and changes in wave-mean flow interactions [*Kodera and Kuroda*, 2002], differences between solar maximum and minimum in the divergence of the Eliassen Palm Flux vector, $\nabla \cdot \mathbf{F}$ (divF), for the two QBO phases are presented in Figure 11. Statistically significant positive $\nabla \cdot \mathbf{F}$ anomalies for the QBO east case in the midlatitude upper stratosphere from July on imply weaker wave-mean flow interaction and hence weaker wave generation during solar maximum conditions that in turn strengthen the west winds (see Figure 10a). Vertically upward propagating planetary waves are reflected poleward in the vicinity of the west wind anomaly and dissipate at higher latitudes (positive anomalies of $\nabla \cdot \mathbf{F}$) where they accelerate the zonal mean flow. Therefore the dissipation region of planetary waves moves poleward and downward with time similar to the westerly wind anomaly (see Figure 10a) and provides a positive

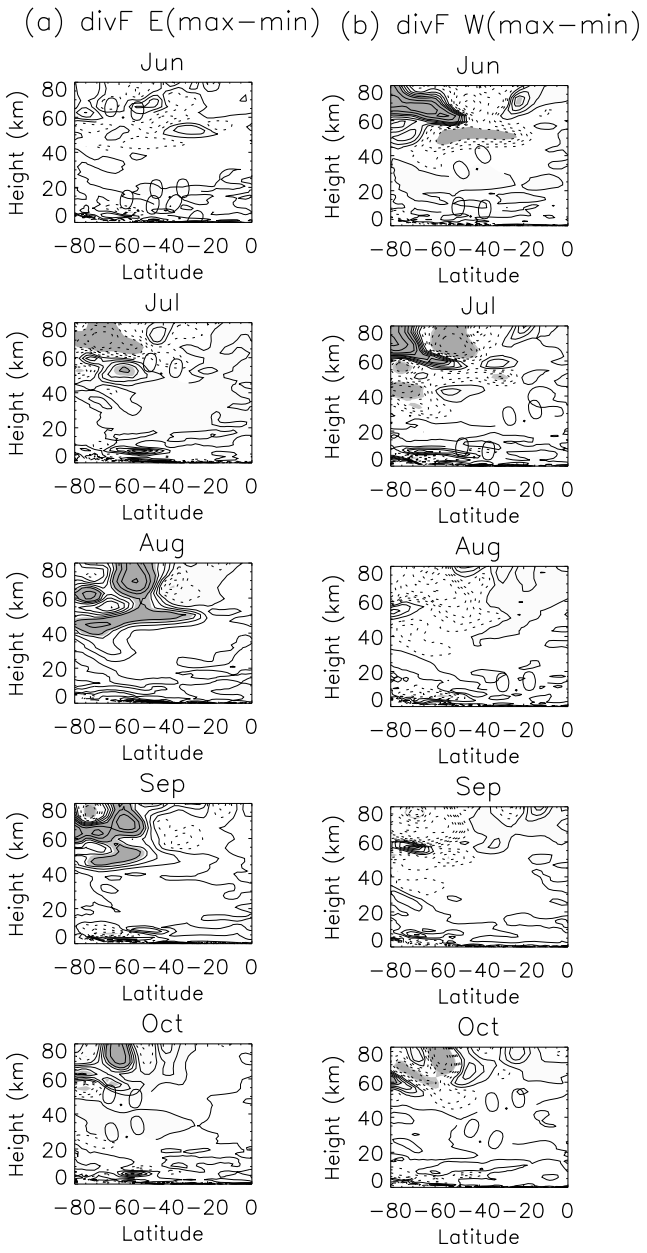

Figure 11. June through October differences between solar maximum and minimum of the divergence of the EP flux vector (divF) for the (a) QBO east (maxE minus minE) and (b) QBO west (maxW minus minW) experiments; shading as in Figure 4.

feedback between the planetary waves and the zonal mean wind anomaly. For the QBO west case, solar induced significant $\nabla \cdot \mathbf{F}$ anomalies occur earlier (June) than for QBO east and are of opposite sign consistent with the zonal-mean wind changes (see Figure 10c). Under QBO east conditions, the weaker convergence at middle to high latitudes in early SH winter induces a weaker poleward BDC during solar maximum and vice versa for QBO west conditions (not shown). This modulation of the BDC leads to the equatorial temperature maximum and corresponding negative anomalies at higher SH latitudes from September through January (see Figures 6 and 7). In WACCM3 the modulation of the PNJ and the BDC are not as clear in the NH as in the SH. Note again that the anomalies in the QBO east case reach further down to the surface than in the QBO west case. The almost opposite response for the two QBO phases agrees very well with observations [e.g., *Labitzke*, 2003] and with other mechanistic model experiments [*Ito et al.*, 2009]. We note that the published results mainly deal with NH winters and WACCM3 is able to reproduce this relation clearly during SH winter only.

5.5. Tropospheric High-Latitude Response

[46] We present the tropospheric response for September since the modulation of the polar night jet and the Brewer Dobson circulation is largest at southern polar latitudes and opposite for the two QBO phases during this time of the year. Similar to the findings by *Matthes et al.* [2006] for the NH, a statistically significant positive Antarctic Oscillation (AAO)-like pattern in geopotential height extends from the stratosphere down to the troposphere and surface in the QBO east experiment (Figure 12, top). The pattern is still significant in the troposphere but weaker compared to the stratospheric pattern. It occurs during the time when the stratospheric zonal-mean zonal wind anomalies extend down to the troposphere (Figure 10a), i.e., during the dynamically controlled part of the winter. In the QBO west experiment the opposite (although nonsignificant) response appears in the middle stratosphere (Figure 12, bottom). The signal is confined to the stratosphere consistent with the wind anomalies (Figure 10c). A similar, although much weaker and less significant, signal is seen during the (also weaker) PNJ modulation in the NH in March (not shown). Here, we do not want to stress the comparison to observations but demonstrate that in the case of a stratospheric modulation of the PNJ and the BDC that extends into the extratropical troposphere, a modulation of the Annular modes (positive AAO pattern in this case) can be obtained.

6. Summary and Discussion

[47] We have demonstrated the effects of a constant, prescribed QBO on the modeled solar signal in the stratosphere and in the high-latitude troposphere by highlighting the importance of the opposing effects of the two QBO phases. A comparison to observations is done where appropriate but it is not the most important aspect of this paper.

[48] The solar signal is small but can be detected in WACCM3. Statistically significant results are mostly confined to the tropical and midlatitude stratosphere. Significant results at high latitudes are obtained in the SH late winter/early spring. The direct solar response in temperature and ozone in the upper stratosphere is in qualitative agreement with other modeling and observational studies independent of the presence of a QBO. During solar maximum temperatures in the tropical stratopause region are about 0.7 K warmer than during solar minimum and ozone increases by 2%–3% in the upper stratosphere.

[49] In the tropical middle and lower stratosphere, the phase of the QBO has a pronounced influence on the vertical structure of the solar signal in temperature and ozone as estimated from the WACCM3 constant forcing simulations (Figure 3). The solar signal in the QBO east and west

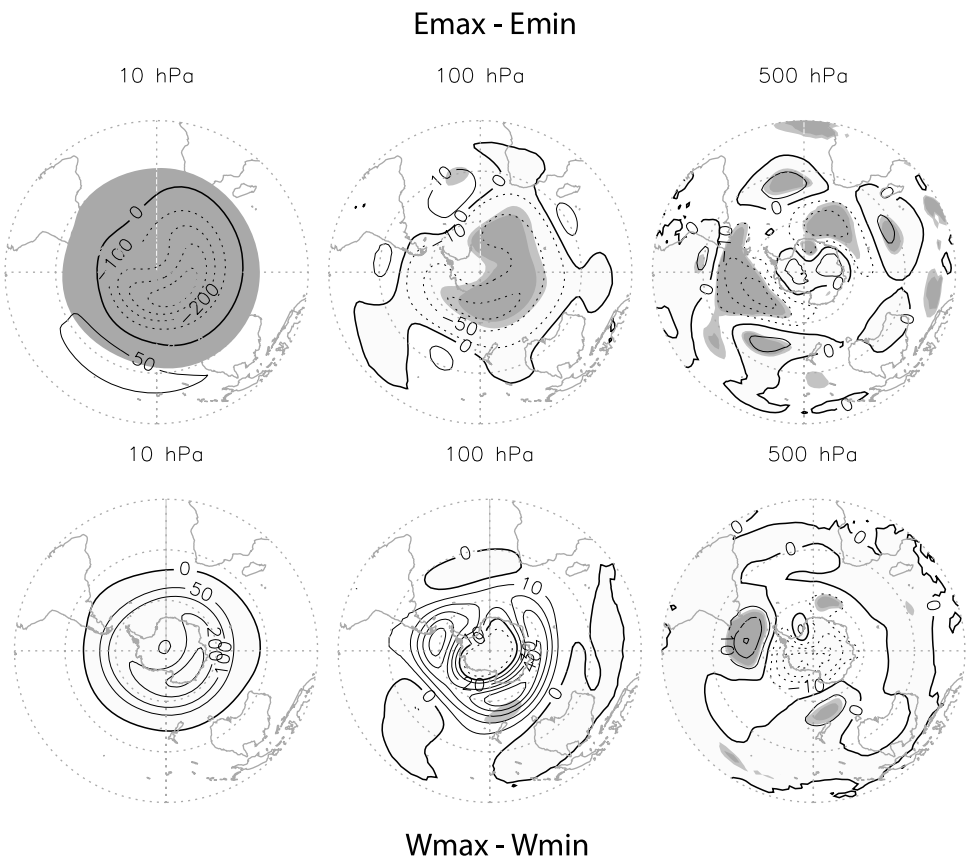

Figure 12. September polar stereographic projection from 20°S to 90°S of the long-term monthly mean geopotential height differences between the solar maximum and minimum for (top) the QBO east experiment and (bottom) the QBO west experiment at 10 hPa, 100 hPa, and 500 hPa, with contour intervals of 10 gpm, 5 gpm, and 2 gpm. Shading as in Figure 4.

experiments is different in the tropics but also at high latitudes (Figures 4–7 and 10–12) and involves large-scale circulation changes in the stratosphere. Mostly dominant westerly wind anomalies at polar latitudes in the QBO east run are consistent with a relative weakening of the BD circulation and therefore relative downwelling and warming and more ozone in the tropical lower stratosphere while mostly east wind anomalies at high latitudes in the QBO west run are consistent with relative upwelling and cooling and less ozone in the tropical lower stratosphere.

[50] The analysis of ozone production, advection and photochemical lifetime (Figures 8 and 9) revealed enhanced ozone production below 25 km that tends to increase the ozone during solar maximum conditions, regardless of the phase of the QBO. Whereas in the QBO west experiment the change in vertical advection removes ozone efficiently and results in little net ozone change in the lower stratosphere, changes in vertical advection are negligible and ozone increases in the lower stratosphere in the QBO east experiment.

[51] The modeled response at polar latitudes (Figures 10–12) is qualitatively consistent with observations [e.g., *Labitzke*, 2003], with another GCM [*Matthes et al.*, 2004, 2006], and with mechanistic model studies [*Ito et al.*, 2009] although the response in WACCM3 is shown for SH winter whereas other studies show it for NH winter. We discuss next why the response in WACCM is smaller during NH winter and compares at least qualitatively with observations during SH winter.

[52] Wave-mean flow interactions are thought to be important for transferring the solar signal from the upper stratosphere to the lower stratosphere and then to the troposphere [e.g., *Kodera and Kuroda*, 2002]. A realistic background climatology is an important prerequisite as noted in earlier studies [*Kodera et al.*, 2003; *Matthes et al.*, 2003]. It is possible that either the mean flow or the wave generation and propagation might not be represented properly in WACCM3. *Richter et al.* [2008] show shortcomings in the background climatology of WACCM3 with a very strong and long lasting SH winter and a less than half as frequent occurrence of stratospheric warmings than in observations during NH winter in the version of WACCM3 used in this study. The relation between shortcomings in the background climatology and the missing of a solar signal propagation is supported by the results from the experiment without a QBO, where only a very weak and nonsignificant poleward-downward movement of the solar signal is found during SH winter and no poleward-downward movement is seen in the NH (not shown). The initial west wind anomaly stays at the same location throughout NH winter. The background climatology in this case shows a strong subtropical jet with large variability almost at the same location throughout the winter (not shown). This unrealistic variability has an effect on wave-mean flow interactions and

might suppress dynamically induced solar changes. The QBO modifies the background wind climatology and leads to a better representation of wave-mean flow interactions in the two QBO cases (Figure 11) as compared to the case without QBO.

[53] The qualitative correspondence of the modeled solar induced signals with observations in the SH could be due to the longer lasting SH winter compared to the NH, so dynamical signals can be more effective or it could be due to a better agreement in the background climatology in the SH compared to the NH winter. It is not clear what role realistic wave representation plays. *Jablonowski and Williamson* [2006] have shown that tropospheric eddies are better represented in GCMs with higher horizontal resolution. We can confirm parts of these findings since we carried out the same set of experiments with a coarser (4° × 5°) model resolution and found that with the finer horizontal resolution (1.9° × 2.5°) version the solar signal and its transfer is more realistic, especially in the SH.

[54] Solar-related changes in the stratosphere lead to changes in the troposphere. During the time of a clear PNJ and BDC modulation a clear AAO-like pattern appears throughout the stratosphere and troposphere during the QBO east case that confirms the modeling study with the noninteractive chemistry model FUB-CMAM in which the ozone distribution was prescribed from a 2-D model [*Matthes et al.*, 2004, 2006] and qualitatively also with several observational studies and a mechanistic model study mentioned above. This agreement as well as additional experiments with WACCM3 under more realistic, time varying forcing (K. Matthes et al., manuscript in preparation, 2010), support the validity of the results presented here. A difference with respect to the results of the FUB-CMAM is that the tropospheric response is very weak in WACCM3. A comparison of the stratospheric wind jet in midlatitudes reveals that the latter is stronger for FUB-CMAM than for WACCM3 (not shown). According to the results from *Sigmond et al.* [2008] this could be a reason for the difference in the tropospheric response that is stronger for the FUB-CMAM than for WACCM3. The constant forcings of the solar cycle and the (prescribed) QBO are another possible limiting factor of the response and might push the model in a permanent extreme case.

7. Conclusions

[55] We have shown results from a set of idealized experiments with the 1.9° × 2.5° horizontal resolution version of WACCM3 with either fixed solar cycle conditions only or fixed solar cycle conditions and fixed, imposed QBO phases, as well as climatological SSTs that help to understand the solar response and especially the role of the QBO for the modulation of the solar signal. The major findings are:

[56] 1. While the model solar response in the upper stratosphere does not depend on the phase of the QBO, the vertical structure of the ozone and temperature model responses in the tropical middle and lower stratosphere are modulated by the QBO such that the solar response is different, sometimes of opposite sign, for the QBO east and west experiments in the tropics and at high latitudes. This is especially evident during SH late winter/early spring for the experiments presented here.

[57] 2. The QBO east experiment shows a statistically significant relative minimum in the solar induced temperature and ozone signal in the middle stratosphere and a statistically significant secondary maximum in the equatorial lower stratosphere. On the other hand, the QBO west experiment shows a relative minimum in the solar temperature and ozone response in the lower stratosphere. This structure is qualitatively consistent with observations [e.g., *Labitzke*, 2003].

[58] 3. We hypothesize that differences in the QBO east and west solar response are related to the corresponding differences in the background climatologies.

[59] 4. The maximum (minimum) in the model temperature and ozone solar signal in the tropical lower stratosphere in the QBO east (west) experiment can also be explained by large-scale circulation changes (modulation of the PNJ and the BDC). The BDC weakens between solar minimum and solar maximum during QBO east and strengthens during QBO west years.

[60] 5. The solar response for the QBO east and west experiments in the lower tropical stratospheric ozone shows coherent but insignificant differences in the production, advection and loss terms. Whereas production and advection contribute to the lower stratospheric ozone maximum during QBO east conditions, the effects tend to cancel each other during QBO west conditions resulting in little net ozone changes.

[61] 6. The results from WACCM3, especially for the QBO east phase, presented here show a vertical structure in the tropical solar response similar to other recent CCM studies [e.g., *Austin et al.*, 2007, 2008; *Matthes et al.*, 2007]. *Austin et al.* [2007, 2008] find this solar signal in experiments with time varying solar cycle and time varying SSTs, *Schmidt et al.* [2010] reproduce it using experiments with fixed solar cycle conditions and climatological SSTs. While these CCM studies do not find a dependence on the presence of an internally generated QBO, the results from WACCM3 clearly show a dependence of the tropical solar signal on the phase of the imposed QBO. Note that the WACCM3 experiment without imposed QBO also produces an enhanced response but it is more pronounced for the QBO east experiment. Since modeling of the QBO is still an outstanding problem for atmospheric models and both internally generated and nudged QBO have limitations, the role of the QBO needs to be further investigated.

[62] 7. The differences in the modeled solar response for the QBO east and west experiments at high latitudes are qualitatively consistent with other GCM [*Matthes et al.*, 2004, 2006] and mechanistic modeling studies [*Ito et al.*, 2009] which in turn qualitatively confirm observations [*Labitzke*, 1987; *Kodera and Kuroda*, 2002]. During solar maximum years the polar stratosphere tends to be cold and undisturbed during QBO east and warm and disturbed during QBO west. In WACCM3 this is especially evident and statistically significant in September during SH winter.

[63] 8. We do not expect a perfect agreement with observations from these highly idealized WACCM3 model simulations. However, the results show that in the case of a PNJ modulation the proposed mechanism from *Kodera and Kuroda* [2002] is working in the stratosphere and a signal

can be detected from the stratosphere to the high latitude troposphere.

[64] A comparison of the constant forcing simulations used in this study with more realistic, time varying forcings are discussed in another set of model experiments (Matthes et al., manuscript in preparation, 2010). Another limitation of the present results are the fixed SSTs that probably reduces the variability and damps the response in the troposphere. This is supported by the results of *Meehl et al.* [2009] which suggest that a fully coupled stratosphere-ocean model is necessary to generate a more realistic solar response.

[65] **Acknowledgments.** This paper is dedicated to the memory of Byron Boville, who initiated the development of WACCM. The authors would like to thank K. Kodera for intense discussions and three anonymous reviewers for very helpful comments that improved the manuscript. We would like to thank L. Gray for providing the equatorial wind data and M. Giorgetta for discussions about the QBO relaxation. K. Matthes was supported by a Marie Curie Outgoing International Fellowship within the Sixth European Community Framework Programme while staying at the National Center for Atmospheric Research and the Freie Universität Berlin. NCAR is operated by the University Corporation for Atmospheric Research under the sponsorship of the National Science Foundation. The calculations for this study were carried out on the Columbia system of the NASA Advanced Supercomputing Facility, Ames Research Center, California, USA.

References

Austin, J., L. L. Hood, and B. E. Soukharev (2007), Solar cycle variations of stratospheric ozone and temperature in simulations with a coupled chemistry-climate model, *Atmos. Chem. Phys.*, *7*, 1673–1706.

Austin, J., et al. (2008), Coupled chemistry climate model simulations of the solar cycle in ozone and temperature, *J. Geophys. Res. 113*, D11306, doi:10.1029/2007JD009391.

Balachandran, N., and D. Rind (1995), Modeling the effects of UV variability and the QBO on the troposphere-stratosphere system. Part I: The Middle Atmosphere, *J. Clim.*, *8*, 2058–2079.

Brasseur, G. (1983), The response of the middle atmosphere to long-term and short-term solar variability: A two-dimensional model, *J. Geophys. Res.*, *98*, 23,079–23,090.

Brasseur, G., and S. Solomon (2005), *Aeronomy of the Middle Atmosphere: Chemistry and Physics of the Stratosphere and Mesosphere*, 3rd ed., Springer, Heidelberg, Germany.

Calisesi, Y., and K. Matthes (2006), The middle atmospheric ozone response to the 11-year solar cycle, *Space Sci. Rev.*, *125*, 273–286.

Camp, C. D., and K. K. Tung (2007), The influence of the solar cycle and QBO on the late winter stratospheric polar vortex, *J. Atmos. Sci.*, *64*, 1267–1283.

Collins, W. D., et al. (2006), The formulation and atmospheric simulation of the Community Atmosphere Model (CAM3), *J. Clim.*, *19*, 2144–2161.

Eyring, V., et al. (2005), A strategy for process-oriented validation of coupled chemistry-climate models, *Bull. Am. Meteorol. Soc.*, *86*, 1117–1133.

Fleming, E. L., S. Chandra, C. H. Jackmann, D. B. Considine, and A. R. Douglass (1995), The middle atmosphere response to short and long term solar UV variations: Analysis of observations and 2D model results, *J. Atmos. Terr. Phys.*, *57*, 333–365.

Fomichev, V. I., J. P. Blanchet, and D. S. Turner (1998), Matrix parameterization of the 15 μm CO_2 band cooling in the middle and upper atmosphere for variable CO_2 concentration, *J. Geophys. Res.*, *103*, 11,505–11,528.

Frame, T. H. A., and L. J. Gray (2010), The 11-year solar cycle in ERA-40 data: An update to 2008, *J. Clim.*, *23*, 2213–2222.

Garcia, R. R., and F. Sassi (1999), Modulation of the mesospheric semiannual oscillation by the quasibiennial oscillation, *Earth Planets Space*, *51*, 563–569.

Garcia, R. R., D. R. Marsh, D. E. Kinnison, B. A. Boville, and F. Sassi (2007), Simulation of secular trends in the middle atmosphere, 1950–2003, *J. Geophys. Res.*, *112*, D09301, doi:10.1029/2006JD007485.

Giorgetta, M. A., E. Manzini, and E. Roeckner (2002), Forcing of the quasi-biennial oscillation from a broad spectrum of atmospheric waves, *Geophys. Res. Lett.*, *29*(8), 1245, doi:10.1029/2002GL014756.

Giorgetta, M. A., E. Manzini, E. Roeckner, M. Esch, and L. Bengtsson (2006), Climatology and forcing of the quasi-biennial oscillation in the MAECHAM5 model, *J. Clim.*, *19*, 3882–3901, doi:10.1175/JCLI3830.1.

Gray, L. J. (2003), The influence of the equatorial upper stratosphere on stratospheric sudden warmings, *Geophys. Res. Lett.*, *30*(4), 1166, doi:10.1029/2002GL016430.

Gray, L. J., E. F. Drysdale, T. J. Dunkerton, and B. N. Lawrence (2001a), Model studies of the interannual variability of the Northern Hemisphere stratospheric winter circulation: The role of the quasi-biennial oscillation, *Q. J. R. Meteorol. Soc.*, *127*, 1413–1432.

Gray, L. J., S. J. Phipps, T. J. Dunkerton, M. P. Baldwin, E. F. Drysdale, and M. R. Allen (2001b), A data study of the influence of the equatorial upper stratosphere on Northern Hemisphere stratospheric sudden warmings, *Q. J. R. Meteorol. Soc.*, *127*, 1985–2003.

Gray, L. J., et al. (2010), Solar influences on climate, *Rev. Geophys.*, doi:10.1029/2009RG000282, in press.

Haigh, J. D. (1994), The role of stratospheric ozone in modulating the solar radiative forcing of climate, *Nature*, *370*, 544–546.

Hamilton, K. P. (2002), On the quasi-decadal modulation of the stratospheric QBO period, *J. Clim.*, *15*, 2562–2565.

Holton, J. R., and H. Tan (1980), The influence of the equatorial quasi-biennial oscillation on the global circulation at 50 mb, *J. Atmos. Sci.*, *37*, 2200–2208.

Holton, J. R., and H. Tan (1982) The quasi-biennial oscillation in the Northern Hemisphere lower stratosphere, *J. Meteorol. Soc. Jpn.*, *60*, 140–148.

Hood, L. L. (2004), Effects of solar UV variability on the stratosphere, in *Solar Variability and Its Effect on the Earth's Atmospheric and Climate System*, *Geophys. Monogr. Ser.*, vol. 141, edited by J. Pap et al., pp. 283–303, AGU, Washington, D. C.

Ito, K., Y. Naito, and S. Yoden (2009), Combined effects of QBO and 11-year solar cycle on the winter hemisphere in a stratosphere-troposphere coupled system, *Geophys. Res. Lett.*, *36*, L11804, doi:10.1029/2008GL037117.

Jablonowski, C., and D. L. Williamson (2006), A baroclinic instability test case for atmospheric model dynamical cores, *Q. J. R. Meteorol. Soc.*, *132*, 2943–2975.

Kinnison, D. E., et al. (2007), Sensitivity of chemical tracers to meteorological parameters in the MOZART3 chemical transport model, *J. Geophys. Res.*, *112*, D20302, doi:10.1029/2006JD007879.

Kodera, K., and Y. Kuroda (2002), Dynamical response to the solar cycle, *J. Geophys. Res.*, *107*(D24), 4749, doi:10.1029/2002JD002224.

Kodera, K., K. Matthes, K. Shibata, U. Langematz, and Y. Kuroda (2003), Solar impact on the lower mesospheric subtropical jet in winter: A comparative study with general circulation model simulations, *Geophys. Res. Lett.*, *30*(D6), 1315, doi:10.1029/2002GL016124.

Kuroda, Y., and K. Kodera (2002), Effect of solar activity on the polar-night jet oscillation in the Northern and Southern Hemisphere winter, *J. Meteorol. Soc. Jpn.*, *80*, 973–984.

Labitzke, K. (1987), Sunspots, the QBO, and the stratospheric temperature in the north polar region, *Geophys. Res. Lett.*, *14*, 535–537, doi:10.1029/GL014i005p00535.

Labitzke, K. (2001), The global signal of the 11-year sunspot cycle in the stratosphere: Differences between solar maxima and minima, *Meteorol. Z.*, *10*, 901–908.

Labitzke, K. (2003), The global signal of the 11-year sunspot cycle in the atmosphere: When do we need the QBO?, *Meteorol. Z.*, *12*, 209–216.

Labitzke, K. (2005), On the solar cycle-QBO relationship: A summary, *J. Atmos. Sol. Terr. Phys.*, *67*, 45–54.

Labitzke, K., and H. Van Loon (1988), Associations between the 11-year solar cycle, the QBO and the atmosphere. Part I: The troposphere and stratosphere in the Northern Hemisphere in winter, *J. Atmos. Terr. Phys.*, *50*, 197–206.

Labitzke, K., M. Kunze, and S. Broennimann (2006), Sunspots, the QBO, and the stratosphere in the north polar region—20 years later, *Meteorol. Z.*, *15*, 355–363.

Lee, H., and A. K. Smith (2003), Simulation of the combined effects of solar cycle, quasi-biennial oscillation, and volcanic forcing on stratospheric ozone changes in recent decades, *J. Geophys. Res.*, *108*(D2), 4049, doi:10.1029/2001JD001503.

Marsh, D. R., and R. R. Garcia (2007), Attribution of decadal variability in lower-stratospheric tropical ozone, *Geophys. Res. Lett.*, *34*, L21807, doi:10.1029/2007GL030935.

Marsh, D., A. Smith, G. Brasseur, M. Kaufmann, and K. Grossmann (2001), The existence of a tertiary ozone maximum in the high-latitude middle mesosphere, *Geophys. Res. Lett.*, *28*, 4531–4534, doi:10.1029/2001GL013791.

Marsh, D. D., R. R. Garcia, D. E. Kinnison, B. A. Boville, F. Sassi, S. C. Solomon, and K. Matthes (2007), Modeling the whole atmosphere

response to solar cycle changes in radiative and geomagnetic forcing, *J. Geophys. Res.*, *112*, D23306, doi:10.1029/2006JD008306.

Matthes, K., K. Kodera, J. D. Haigh, D. T. Shindell, K. Shibata, U. Langematz, E. Rozanov, and Y. Kuroda (2003), GRIPS solar experiments intercomparison project: Initial results, *Pap. Meteorol. Geophys.*, *54*, 71–90.

Matthes, K., U. Langematz, L. J. Gray, K. Kodera, and K. Labitzke (2004), Improved 11-year solar signal in the Freie Universität Berlin Climate Middle Atmosphere Model (FUB-CMAM), *J. Geophys. Res.*, *109*, D06101, doi:10.1029/2003JD004012.

Matthes, K., Y. Kuroda, K. Kodera, and U. Langematz (2006), Transfer of the solar signal from the stratosphere to the troposphere: Northern winter, *J. Geophys. Res.*, *111*, D06108, doi:10.1029/2005JD006283.

Matthes, K., K. Kodera, L. Gray, J. Austin, A. Kubin, U. Langematz, D. Marsh, J. McCormack, K. Shibata, and D. Shindell (2007), Report on the first SOLARIS workshop: 4–6 October 2006, Boulder, Colorado, USA, *SPARC Newsl.*, *28*, 19–22.

McCormack, J. P. (2003), The influence of the 11-year solar cycle on the quasi-biennial oscillation, *Geophys. Res. Lett.*, *30*(22), 2162, doi:10.1029/2003GL018314.

Meehl, G. A., J. M. Arblaster, K. Matthes, F. Sassi, and H. van Loon (2009), Amplifying the Pacific climate system response to a small 11-year solar cycle forcing, *Science*, *325*, 1114–1118, doi:10.1126/science.117287.

Pascoe, C. L., L. J. Gray, S. A. Crooks, M. N. Juckes, and M. P. Baldwin (2005), The quasi-biennial oscillation: Analysis using ERA-40 data, *J. Geophys. Res.*, *110*, D08105, doi:10.1029/2004JD004941.

Randel, W. J., and F. Wu (2007), A stratospheric ozone profile data set for 1979–2005: Variability, trends, and comparisons with column ozone data, *J. Geophys. Res.*, *112*, D06313, doi:10.1029/2006JD007339.

Randel, W. J., et al. (2009), An update of observed stratospheric temperature trends, *J. Geophys. Res.*, *114*, D02107, doi:10.1029/2008JD010421.

Richter, J. H., F. Sassi, R. R. Garcia, K. Matthes, and C. Fisher (2008), Dynamics of the middle atmosphere as simulated by the Whole Atmosphere Community Climate Model, version 3 (WACCM3), *J. Geophys. Res.*, *113*, D08101, doi:10.1029/2007JD009269.

Roble, G. R. (1995), Energetics of the mesosphere and thermosphere, in *The Upper Mesosphere and Lower Thermosphere: A Review of Experiment and Theory*, *Geophys. Monogr. Ser.*, vol. 87, edited by R. M. Johnson and T. L. Killen, pp. 1–21, AGU, Washington, D. C.

Roble, G. R., and E. C. Ridley (1987) An auroral model for the NCAR thermospheric general circulation model (TGCM), *Ann. Geophys., Ser. A*, *5*, 369–382.

Salby, M., and P. Callaghan (2000), Connection between the solar cycle and the QBO: The missing link, *J. Clim.*, *13*, 2652–2662.

Salby, M., and P. Callaghan (2004) Evidence of the solar cycle in the general circulation of the stratosphere, *J. Clim.*, *17*, 34–46.

Salby, M., and P. Callaghan (2006), Relationship of the quasi-biennial oscillation to the stratospheric signature of the solar cycle, *J. Geophys. Res.*, *111*, D06110, doi:10.1029/2005JD006012.

Scaife, A., N. Butchart, C. Warner, D. Staniforth, W. Norton, and J. Austin (2000), Realistic quasi-biennial oscillation in a simulation of the global climate, *Geophys. Res. Lett.*, *27*, 3481–3484.

Schmidt, H., and G. Brasseur (2006), The response of the middle atmosphere to solar cycle forcing in the Hamburg Model of the Neutral and Ionized Atmosphere, *Space Sci. Rev.*, *125*, 345–356.

Schmidt, H., G. P. Brasseur, and M. A. Giorgetta (2010), Solar cycle signal in a general circulation and chemistry model with internally generated quasi-biennial oscillation, *J. Geophys. Res.*, *115*, D00I14, doi:10.1029/2009JD012542.

Shibata, K., and M. Deushi (2005), Partitioning between resolved wave forcing and unresolved gravity wave forcing to the quasi-biennial oscillation as revealed with a coupled chemistry-climate model, *Geophys. Res. Lett.*, *32*, L12820, doi:10.1029/2005GL022885.

Shindell, D., D. Rind, N. Balachandran, J. Lean, and P. Lonergan (1999), Solar cycle variability, ozone and climate, *Science*, *284*, 305–308.

Sigmond, M., J. F. Scinocca, and P. J. Kushner (2008), Impact of the stratosphere on tropospheric climate change, *Geophys. Res. Lett.*, *35*, L12706, doi:10.1029/2008GL033573.

Smith, A. K., and K. Matthes (2008), Decadal-scale periodicities in the stratosphere associated with the solar cycle and the QBO, *J. Geophys. Res.*, *113*, D05311, doi:10.1029/2007JD009051.

Solomon, S. C., and L. Qian (2005), Solar extreme-ultraviolet irradiance for general circulation models, *J. Geophys. Res.*, *110*, A10306, doi:10.1029/2005JA011160.

Soukharev, B. E., and L. L. Hood (2001), Possible solar modulation of the equatorial quasi-biennial oscillation: Additional statistical evidence, *J. Geophys. Res.*, *106*, 14,855–14,868, doi:10.1029/2001JD900095.

Soukharev, B. E., and L. L. Hood (2006), Solar cycle variation of stratospheric ozone: Multiple regression analysis of long-term satellite data sets and comparisons with models, *J. Geophys. Res.*, *111*, D20314, doi:10.1029/2006JD007107.

Tilmes, S., R. R. Garcia, D. E. Kinnison, A. Gettelman, and P. J. Rasch (2009), Impact of geoengineered aerosols on the troposphere and stratosphere, *J. Geophys. Res.*, *114*, D12305, doi:10.1029/2008JD011420.

van Loon, H., and K. Labitzke (2000), The influence of the 11-year solar cycle on the stratosphere below 30 km: A review, *Space Sci. Rev.*, *94*, 259–278.

World Meteorological Organization (2007), Scientific assessement of ozone depletion: 2006, *Global Ozone Res. and Monit. Proj. Rep. 50*, Geneva, Switzerland.

R. R. Garcia, D. E. Kinnison, D. R. Marsh, and S. Walters, National Center for Atmospheric Research, PO Box 3000, Boulder, CO 80307, USA.

K. Matthes, Deutsches GeoForschungsZentrum, Telegrafenberg, D-14473 Potsdam, Germany. (matthes@gfz-potsdam.de)

F. Sassi, Naval Research Laboratory, 4555 Overlook Ave. SW, Washington, DC 20375, USA.